Extraordinary transmittance in three-dimensional crater, pyramid, and hole-array structures prepared through reversal imprinting of metal films

H. L. Chen*, S. Y. Chuang, W. H. Lee, S. S. Kuo, W. F. Su, S. L. Ku[a,b], and Y. F. Chou[b]

Department of Materials Science and Engineering, National Taiwan University, Taipei, Taiwan
[a]Department of Optics and Photonics/Thin Film Technology Center, National Central University
[b]Material & Electro-Optics Research Division, Chung-Shan Institute of Science & Technology, Taiwan
**Corresponding author: hsuenlichen@ntu.edu.tw*

Abstract: We used a reversal imprinting-in-metal (RIM) process to fabricate various three-dimensional (3D) metal structures under low pressure. Molds featuring different shapes were used to pattern various sub-wavelength metal structures, including pyramidal, hole-array, and crater-like structures. Refractive index matching and cavity effects both enhanced the degree of transmission of these structured metal films. The crater-like structure appears to be a promising material because of the unique properties imparted by the elongated and gradually tapering spacing of its cavities. From both near-field simulations and experimentally obtained optical spectra, we found that the cavity effect in the crater-like structure led to significantly enhanced transmission of the optical intensity. Thus, this RIM process allows the ready fabrication of various two- and three-dimensional metallic structures for use in surface plasmon-based devices.

OCIS codes: (160.4760) Optical properties; (220.3740) Lithography; (240.6680) Surface plasmons; (220.4000) Microstructure fabrication

References and links

1. T. W. Ebbesen, H. J. Lezec, H. F. Ghaemi, T. Thio, P. A. Wolff, "Extraordinary optical transmission through sub-wavelength hole arrays," Nature **391**, 667-669 (1998).
2. J. B. Pendry, L. Martyn-Moreno, F. J. Garcia-Vidal, "Mimicking Surface plasmons with structured surfaces," Science **305**, 847-848 (2004).
3. H. Gao, J. Joel Henzie, T.Odom, "Direct evidence for surface plasmon-mediated enhanced light transmission through metallic nanohole arrays," Nano Lett. **6**, 2104-2108 (2006).
4. W. C. Liu, "High sensitivity of surface plasmon of weakly-distorted metallic surfaces," Opt. Express **13**, 9766-9773 (2005). http://www.opticsinfobase.org/oe/abstract.cfm?URI=oe-13-24-9766
5. P. Andrew, W. L. Barnes, "Energy transfer across a metal film mediated by surface plasmon polaritons," Science **306**, 1002-1005 (2004).
6. J. M. Brockman, B. P. Nelson, R. M. Corn, "Surface plasmon resonance imaging measurements of ultrathin organic films," Annu. Rev. Phys. Chem. **51**, 41-63 (2000).
7. J. Homola, *Surface Plasmon Resonance Based Sensors* (Springer, 2006).
8. T. H. Reilly, J. van de Lage, R. C. Tenent, A. J. Morfa and K. L.Rowlen, "Surface-plasmon enhanced transparent electrodes in organic photovoltaics," Appl. phys. Lett. **92**, 243304 (2008).
9. S. M. Orbons, A. Roberts, "Resonance and extraordinary transmission in annular aperture arrays," Opt. Express **14**, 12623-12628 (2006). http://www.opticsinfobase.org/oe/abstract.cfm?URI=oe-14-26-12623
10. N. Bonod, S, Enoch, L. Li, E. Popov, M. Neviere, "Resonant optical transmission through thin metallic films with and without holes," Opt. Express **11**, 482-490 (2003). http://www.opticsinfobase.org/oe/abstract.cfm?URI=oe-11-5-482
11. B. F. Bai, L. F. Li, L. J. Zeng, "Experimental verification of enhanced transmission through two-dimensionally corrugated metallic films without holes," Opt. Lett. **30**, 2360-2362 (2005).
12. S. Wedge, I. R. Hooper, I. Sage, W. L. Barnes, "Light emission through a corrugated metal film: The role of cross-coupled surface plasmon polaritons," Phys. Rev. B **69**, 245418 (2004).

#104420 - $15.00 USD Received 21 Nov 2008; revised 17 Jan 2009; accepted 18 Jan 2009; published 27 Jan 2009

13. Z. M. Zhu, T. G. J. Brown, "Nonperturbative analysis of cross coupling in corrugated metal films," Opt. Soc. Am. A **17**, 1798-1806 (2000).
14. I. Avrutsky, Y. Zhao, V. Kochergin, "Surface-plasmon-assisted resonant tunneling of light through a periodically corrugated thin metal film," Opt. Lett. **25**, 595-597 (2005).
15. S. Y. Chuang, H. L. Chen, S. S. Kuo, Y. H. Lai, C. C. Lee, "Using direct nanoimprinting to study extraordinary transmission in textured metal films," Opt. Express **16**, 2415-2422 (2008). http://www.opticsinfobase.org/oe/abstract.cfm?URI=oe-16-4-2415
16. D. Suh, J. Rhee, H. H. Lee, "Bilayer reversal imprint lithography direct metal-polymer transfer," Nanotechnology **15**, 1103-1107 (2004).
17. J. W. Kim, K.Y. Yang, S. H. Hong, H. Lee, "Formation of Au nano-patterns on various substrates using simplified nano-transfer printing method," Appl. Surf. Sci. **254**, 5607-5611 (2008).
18. J.Zaumseil, A. Meitl, J. W. P. Hsu, B.R. Acharya, K.W. Baldwin, Y. L. Loo, J.A. Rogers, "Three dimensional and multilayer nanostructures formed by nanotransfer printing," Nano Lett. **3**, 1223-1227 (2003).
19. Y. L. Loo, D. V. Lang, J. A. Rogers, J. W. P. Hsu, "Electrical contacts to molecular layers by nanotransfer printing," Nano Lett. **3**, 913-917 (2003).
20. C. Peng, B. L. Cardozo, S. W. Pang, "Three-dimensional metal patterning over nanostructures by reversal imprint," J. Vac. Sci. Tech. B **26**, 632-635 (2008).
21. J. Y. Ma, S. Y. Liu, D. W. Zhang, J. K. Yao, C. Xu, J. D. Shao, Y. X. Jin, Z. X. Fan, "Study of the surface plasma transmission properties of a Fabry-Perot resonator by numerical simulation," J. Opt. A **10**, 035002 (2008)
22. H. Iu, J. Li, H. C. Ong, J. T. K. Wan, "Surface plasmon resonance in two-dimensional nanobottle arrays," Opt. Express **16**, 10294-10302 (2008). http://www.opticsinfobase.org/oe/abstract.cfm?URI=oe-16-14-10294
23. E. D. Palik, *Handbook of optical constants of solids* (Academic, 1985)

1. Introduction

Surface plasma resonance (SPR) phenomena are at the core of many fascinating studies in physics [1-4], chemistry [5,6] and surface plasmon resonance sensors [7]. Recent advances in the preparation of sub-wavelength structures have enabled control over their SPR properties, thereby allowing explorations of potential specific applications in semi-transparent electrodes [8]. SPR-induced extraordinary transmittance has attracted much attention [1-3,9], it occurs when the transmission of a metallic material featuring specific sub-wavelength structures is much higher than that expected from classic diffraction theory. The phenomenon is attributed to the coupling of incident light to the surface plasmons (SPs) on the structured metal film. The interaction between the electric field and the surface charges that constitute the SP is obtained by solving Maxwell's equations, yielding the following SP dispersion relation:

$$k_{sp} = k_0 \sqrt{\frac{\varepsilon_d \varepsilon_m}{\varepsilon_d + \varepsilon_m}} \tag{1}$$

where k_{sp} is the frequency-dependent SP wave vector, k_0 is the wave vector of the incident light in free space, and ε_d and ε_m are the permittivities of the dielectric and the metal material, respectively. The difference between k_{sp} and k_0 of the same frequency is associated with the biding of the SP to the surface. Generation of the SPR must occur to compensate for this mismatch. Introduction of sub-wavelength structures allows the momentum of the SPR to be augmented or reduced through Bragg scattering from the periodic structure, as indicated in the following equation:

$$k_{sp} = k_0 \sin\theta \pm n k_g \tag{2}$$

where k_g is the grating wave vector, $k_0 \sin\theta$ is the in-plane wave vector, θ is the polar angle of the incident light, and n is an integer defining the order of the scattering. There are two main approaches through which the missing momentum can be provided for the extra wave-vector generating SPs: (i) sub-wavelength hole-arrays allowing scattering from a topological defect on the metal surface or (ii) the use of periodic corrugation in the metal surface. In sub-wavelength structures, incident light of certain wavelengths passes through metal hole-arrays having specific diameters and periods.

#104420 - $15.00 USD Received 21 Nov 2008; revised 17 Jan 2009; accepted 18 Jan 2009; published 27 Jan 2009

Continuous metal films featuring appropriate degrees of corrugation can exhibit extraordinary transmittance [10-15]. When a metal film is sufficiently thin, the SP modes of the two surfaces can overlap and interact on both sides of the patterned metal film. As a result, extraordinary transmission phenomena can also be found in continuously corrugated metal films that do not feature perforated hole-arrays. Metal films having sinusoidal profiles can be fabricated using conventional holographic techniques. Generally, it is difficult to control the depth and shape of the sinusoidal metal profiles when using holographic lithography because of nonlinearity of the resist sensitivity. Recently, we reported a nanoimprinting-in-metal (NIM) method for patterning metal films with sinusoidal profiles of various depths [15]. SPR phenomena allowed energy coupling to the other side of such sinusoidal metal films, causing a dramatic increase in the transmission. The ability to use NIM to fabricate various three-dimensional (3D) metal structures is limited, however, by the mechanical strength of the thin metal film. Furthermore, relatively little research has been conducted on 3D metals featuring sub-wavelength structures other than hole-arrays or sinusoidal patterns [9].

In this study, we prepared various metal structures, such as craters, to further investigate extraordinary transmission phenomena. Combining hole-arrays with sinusoidal profiles leads to this certain type of 3D metal structure that possesses unique optical characteristics. These complicated structures are almost impossible to fabricate using conventional lithographic methods. Here we describe an imprinting approach, using a "reversal imprinting in metal" (RIM) technique, for patterning various 3D metal structures. This technique is simple to perform, suitable for various types of metals, and allows the patterning of various profiles in metal structures. Conventional processes for generating 3D metal structures generally involve multiple deposition, lithography, and etching steps that can be laborious and expensive. Reversal imprint techniques based on nanoimprinting provide simple and inexpensive patterning capabilities that can generate certain types of 3D structures [16-20]. To date, most approaches using RIM have focused on the fabrication of nano-channels [18, 20]. In this paper, we demonstrate the fabrication of complicated 3D metallic structures featuring a variety of patterns through RIM processing using various shaped molds. Some of these metallic structures have potential use in SPR-based and photonics devices. Moreover, we have observed extraordinary transmittance assisting through cavity- and refractive index-matching effects in our sub-wavelength hole-array structures.

2. Simulation and Experiment Setup

In the RIM approach, a silicon mold having a chemically modified surface is coated with a metal film and then transferred onto a UV curable polymer-coated substrate (Fig. 1). First, the UV curable resist (SU-8, Microchem) was spin-coated onto a glass substrate. Next, thin film of gold was deposited onto a surfactant (1H,2H,2H-fluorooctyltrichlorosilane)-coated silicon mold, which then directly contacted with resist. In the thermal deposition process of gold film, the deposition rate was a few Å per second and performed at room temperature within 10^{-6} mTorr pressure. The imprint process was performed using a conventional imprint instrument. Moderate pressure and UV light radiation were applied to the resist-coated substrate. The adhesion between the gold film and the resist was effected through the monomer units undergoing crosslinking to form a hard epoxy under exposure to UV light. Finally, the silicon mold was removed to reveal the designed metal patterns on the resist-coated substrate. The silicon molds were fabricated using electron beam lithography (Leica, Weprint-200) followed by reactive ion etching (RIE). A high density plasma reactive ion etching (HDP-RIE) system (Duratek, Mutiplex Cluster) equipped with an inductively coupled plasma (IPC) source was used to fabricate the various profiles of the molds. The bias and RF power used for HDP-RIE were critical parameters for controlling the surface profiles of molds. As indicated in Fig. 1(a), the two-dimensional (2D) corrugated gold films were readily fabricated through RIM processing using a pyramidal mold. Figure 1(b) displays hole-arrays in a gold film patterned with a hole-array mold. Images of patterned metal films were measured using a scanning electron microscope (SEM; Hitachi, S-4000). Transmission spectra of the structured metal films were acquired using an optical spectrometer (Hitachi, U-4100). For near-field analysis,

#104420 - $15.00 USD Received 21 Nov 2008; revised 17 Jan 2009; accepted 18 Jan 2009; published 27 Jan 2009

the finite-difference time domains (FDTD) method was used to determine the optical behavior of the transmission of light through the various nanostructures of the thin gold film. The optical constants of materials used in simulations are acquired from established database [23].

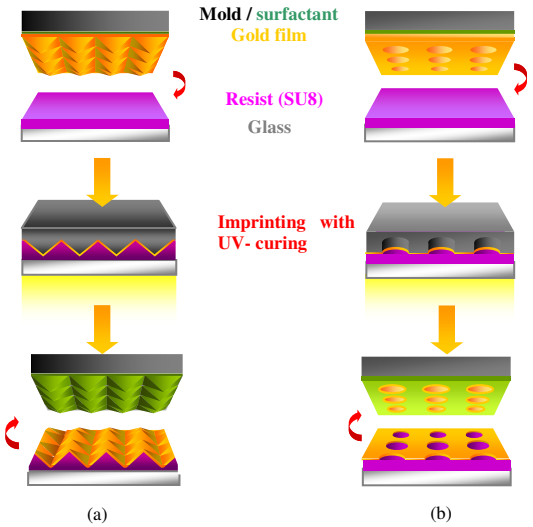

Fig. 1. Schematic representation of the RIM process for the preparation: (a) a two-dimensional corrugated metal film and (b) a metal hole-array structure.

One of greatest advantages of the RIM process is that metal films featuring various profiles can be readily fabricated and replicated from various molds subjected to low imprinting pressures. Thin gold films can be transferred from the surfactant-coated mold to the resist-coated substrate under extremely low pressure (<0.1 MPa) because of the surface energy difference between the surfactant and adhesion promotion layer of the UV-cured resist. In this study, we used an SU-8 film as the adhesion promotion layer for the metal film in our reversal imprint process. Figure 2 presents images of the molds and their transferred metal structures after performing the RIM process. Figure 2(a) reveals the structure of a pyramid-shaped mold having a height of 120 nm and a period of 400 nm. After performing the RIM process, we obtained a corrugated gold film having a period of 400 nm (Fig. 2(b)). This RIM technology can be used to prepare metal films featuring various configurations; the contact surface profile between the gold film and the resist determines the morphology of the transferred metal film. Figure 2(c) displays the image of a silicon mold having a feature depth of 900 nm, a hole diameter of 400 nm, and a period of 800 nm. Patterning of the contact area between the gold film and the polymer provided a flat gold film possessing periodic holes (Fig. 2(d)). We attribute to two main factors to the relative ease with which we used the RIM approach to fabricate the various profiles in these thin gold films: (i) the surface profiles of the areas in contact with the resist during the imprinting process and (ii) the thickness of thin metal film on the molds' sidewall. That is to say, the contact profile and thickness of thin gold film on the molds' sidewall determine which parts of the gold film become transferred. The pattern of the reversal imprint is limited by the adherent ability provided by the UV-cured polymer.

#104420 - $15.00 USD Received 21 Nov 2008; revised 17 Jan 2009; accepted 18 Jan 2009; published 27 Jan 2009

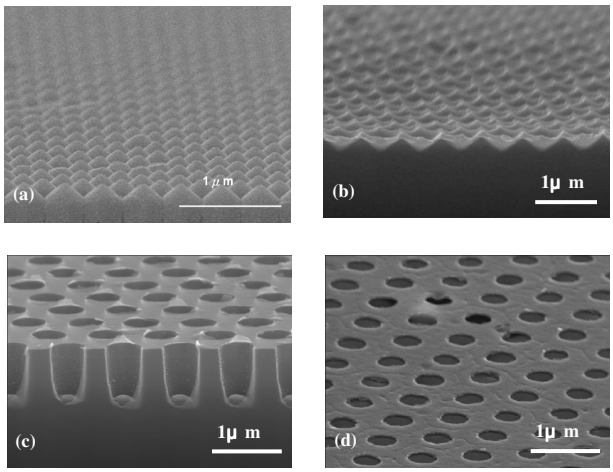

Fig. 2. SEM images of silicon molds and structures of gold films patterned using the RIM process. (a) 2D corrugated silicon mold; (b) corrugated thin gold film; (c) deep hole-array mold; (d) gold hole-array structure.

Figure 3(a) presents a schematic representation of a 3D crater structure fabricated using the RIM process. For the fabrication of such a 3D metal structure, we combined the topographic characteristics of the molds in Fig. 2(a) and 2(c). A sharp mold possessing features having a height of 1 μm and a period of 800 nm was used in the imprinting processes. We employed an HDP-RIE system to fabricate molds exhibiting various profiles. The mold displayed in Fig. 3(b) was similar to that in Fig. 2(c), but it featured sharper structures on the top of its features. The height of each sharp part of the mold was ca. 200 nm. After reversal imprinting, Fig. 3(d) reveals that we obtained a gold crater structure featuring hole-arrays having a thickness of 45 nm and a height of 200 nm. It is clear that through a judicious selection of the molds, we could use this simple RIM method to pattern complicated 2D and 3D metal structures.

3. Results and discussion

To determine the optical properties of the various metal structures prepared using the RIM technique, we used an optical spectrometer to characterize and compare the extraordinary transmission phenomena exhibited by three specific structures: a 2D corrugated film (Fig. 2(b)), a hole array (Fig. 2(d)), and a crater structure (Fig. 3(c)).

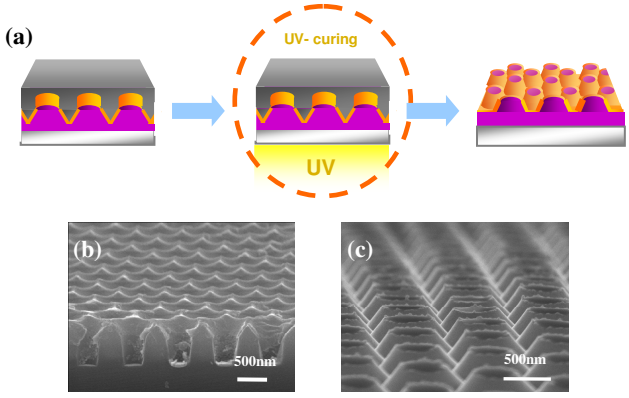

Fig. 3. (a) Schematic representation of a crater-like structure fabricated using the RIM process. (b, c) SEM images of (b) a sharp silicon mold and (c) a gold crater structure.

#104420 - $15.00 USD Received 21 Nov 2008; revised 17 Jan 2009; accepted 18 Jan 2009; published 27 Jan 2009

Figure 4 displays the transmittance spectra of 45-nm gold films with and without corrugated structures. Since the curvature of corrugated gold structures is a key factor for extraordinary transmittance [15], we set suitable architecture for corrugated gold films which lead to significant SPR induced phenomena. A SPR transmittance enhancement can be obtained in the corrugated gold films having a period of 400nm and a height of 120nm which is attributed to its larger curvature than the larger period structures. The spectrum of the flat gold film features only the intrinsic peak for gold at 510 nm. The transmission of this intrinsic signal varied only with respect to the thickness of the gold film. The transmission spectrum of the corrugated gold film having a period of 400 nm reveals that SPR, induced by the periodic metal structure, caused the transmittance peak to shift to 530 nm, with the peak intensity increasing to 27.2% from the value of 19.5% of the flat gold film. We attribute this slight enhancement in the degree of transmission to the mismatch in the refractive indexes on the two sides of the corrugated gold film (i.e., the two-layer structure air/corrugated gold film/resist). This refractive index mismatch leads to insignificant overlap of SPR coupling on the two sides of the patterned gold film. To increase the degree of extraordinary transmittance, we coated a resist layer onto the corrugated gold film. The transmission of the corrugation gold film covered with SU-8 (i.e., the three-layer structure resist/corrugated gold film/resist) increased dramatically to 46.2% at 600 nm as a result of refractive index matching. That is, the SPR on each side of the corrugated gold film exhibited the same wave vector; overlap of these two SPR signals resulted in strong coupling of light. Therefore, the refractive indices at the two surfaces of a patterned gold film play an important role in affecting the degree of SPR-induced extraordinary transmittance.

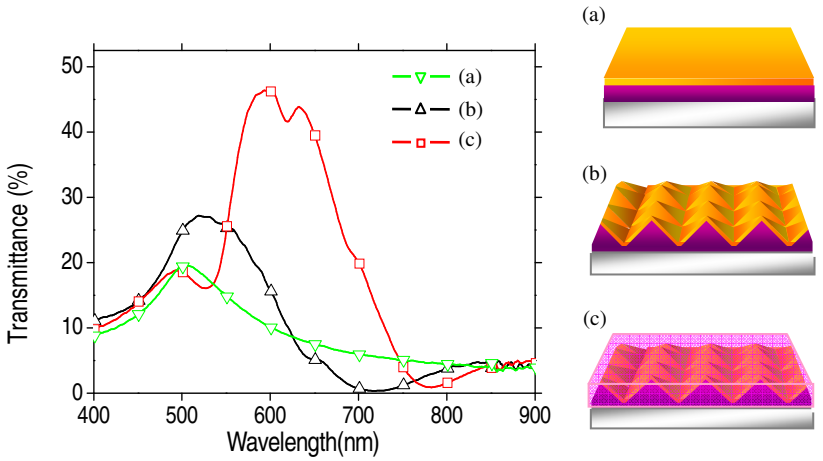

Fig. 4. Transmittance spectra of a 45-nm-thick (a) flat gold film, (b) corrugated gold film, and (c) corrugated gold film covered with resist.

The cavity effect results from an optical field confined within the cavities of metallic or dielectric structures [3,21]. To determine the role of the cavity effect in our extraordinary transmission phenomena, we investigated the behavior of the metal hole arrays filled with air or resist, using the FDTD approach. FDTD simulations reveal the electromagnetic fields over the entire computational domain as they evolve over time, providing animated displays of the electric field's movement through the model. We used FDTD calculations to analyze the cavity effect on our patterned metal films. Figure 5(a) reveals that a plane wave having a wavelength of 1350 nm propagated from the resist (bottom) side of the structure (air/empty gold hole array/resist) through a 45-nm-thick hole array having a hole-diameter of 400 nm and a period of 800 nm to the air side. In the simulation setup, the optical constants (n, k) of the gold film and resist at 1350nm are (0.458, 9.72) and (1.58, 0), respectively. Because of the

#104420 - $15.00 USD Received 21 Nov 2008; revised 17 Jan 2009; accepted 18 Jan 2009; published 27 Jan 2009

refractive index mismatch, we observed lower electric field intensity both in the empty cavities and on the air (top) side of the structure. Figure 5(b) displays the electric field intensity distribution of a resist-filled gold hole-array structure of the same thickness, hole diameter, and period. We observe that a stronger electric field was localized in the cavities after matching of the refractive indices.

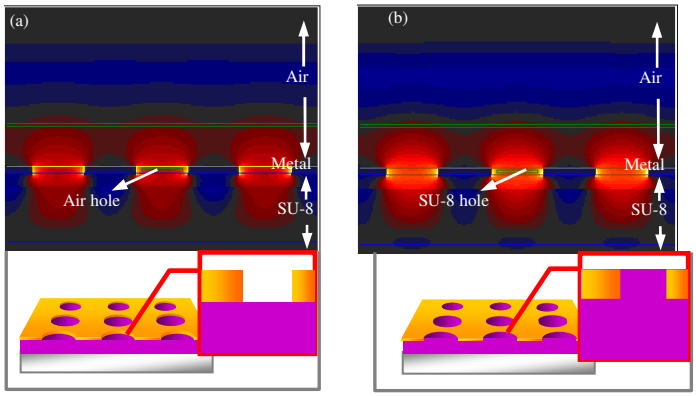

Fig. 5. FDTD diagrams of (a) an empty gold hole-array and (b) a resist (SU-8)-filled hole-array; thickness, 45 nm; hole diameter, 400 nm; period, 800 nm.

Next, we investigated how the cavities of the gold hole-array structure could be filled with resist during the RIM process by applying a suitable imprinting pressure. Figure 6(a) displays the SEM image of an empty-cavity gold hole-array structure, fabricated through RIM, having a hole diameter of 400 nm and a period of 800 nm. Figure 6(b) displays a gold hole-array featuring cavities filled with resist at a pressure of 7.5 MPa. During this the imprinting process, the resist flowed into holes of the mold prior to UV exposure. Thus, merely applying a moderate pressure allows the cavities of these gold hole-array structures to be filled with resist. Therefore, experimental comparisons can be readily made between the air/empty hole/substrate and the air/resist-filled hole/substrate structures prepared through RIM processing without changing the nature of the air ambient.

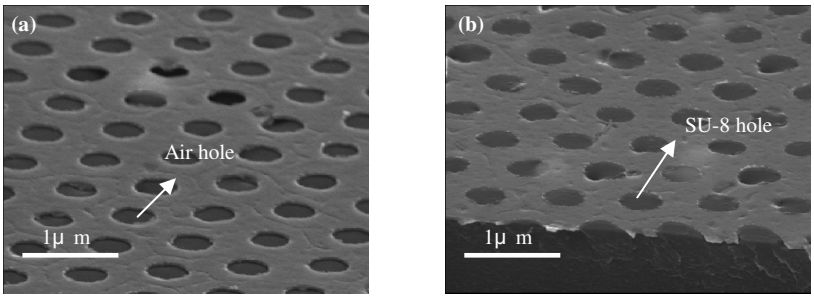

Fig. 6. Gold films on a glass substrate coated with SU-8, possessing (a) periodic empty holes and (b) periodic holes filled with SU-8.

Figure 7 displays transmission spectra of the empty and resist-filled gold hole-array structures. In the empty hole-array structure (the two-layer structure air/empty hole-array/resist), the transmission peak for the SPR mode of the air–gold interface appeared at 1325 nm with an intensity of 37.6%. In the corresponding resist-filled hole-array structure, the peak transmittance increased to 50.8% at the same wavelength because of the cavity effect;

#104420 - $15.00 USD Received 21 Nov 2008; revised 17 Jan 2009; accepted 18 Jan 2009; published 27 Jan 2009

i.e., the resist filling the holes increases the effective optical path length of the cavities and, therefore, the amplitude of the SP waves is more confined within the holes. Moreover, because the SPR peaks of the empty and resist-filled hole-arrays resonated at the same wavelength, we conclude that the same SPR modes were induced by the same interfacial medium (air–gold). The transmittance of the hole-array structure coated with an additional resist layer (the three-layer structure resist/resist-filled hole-array/resist) was higher transmission: 57.8% at 1465 nm. This three-layer structure induced a stronger SPR as a result of the index matching effect. The red-shift in the wavelength of the SPR implies that the SPR mode changed to the resist–gold mode on the surface of three-layer structure.

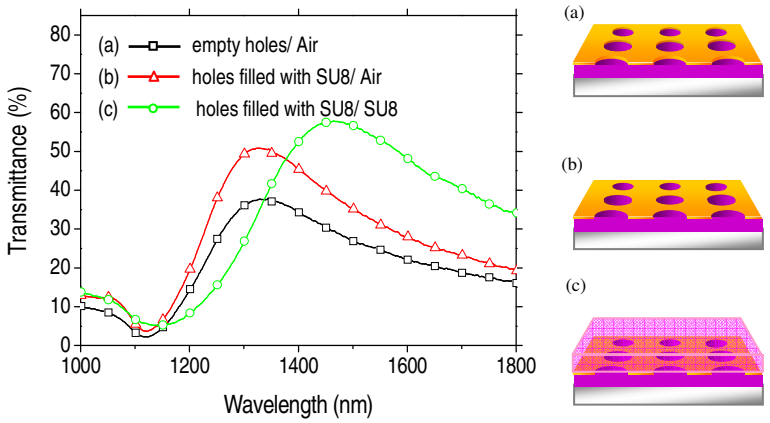

Fig. 7. Transmittance spectra of (a) an empty hole-array structure, (b) a resist-filled hole-array structure, and (c) a three-layer resist-filled hole-array structure.

Our results above suggested that increasing the transmittance in hole-array structures required the use of the cavity effect. We suspected that a 3D crater-type hole-array structure having the same film thickness of 45nm would provide the elongation and gradual changing of the spacing in the cavity required to confine more SP waves within the holes. Figure 8(a) reveals that a plane wave having a wavelength of 1350 nm propagated through the crater structure having the same hole diameter, period, optical constants, and height of 200 nm. A significant electric field amplitude appeared in each cavity. Enhanced confinement of the optical field in the crater structure allows more energy to pass through the sub-wavelength holes. Figure 8(b) displays the simulated transmission spectra of various structures in the near-field regime. The transmitted optical field was small for the empty hole-array having a depth of 45 nm. A slight enhancement in the optical field intensity occurred for the empty hole-array after increasing the depth of the holes to 100 nm. A refractive index matching effect was evident in the hole-array filled with the resist, resulting in enhanced transmission. The red-shift of this SPR peak was caused by the refractive index difference between the air and the resist. Moreover, we observed a higher electric field intensity in a crater structure possessing elongated cavity walls. The maximum electric field intensity of the 3D crater-array structure was 26.9. For the same height (200 nm), the electric field intensity of the hole-array structure dropped dramatically to 6.91. Thus, the maximum value of the electric field intensity of the crater hole-array structure was nearly 3.9 times greater than that of the empty hole-array structure in the near-field regime, revealing that the gold crater structure provides a significantly enhanced transmission.

#104420 - $15.00 USD Received 21 Nov 2008; revised 17 Jan 2009; accepted 18 Jan 2009; published 27 Jan 2009

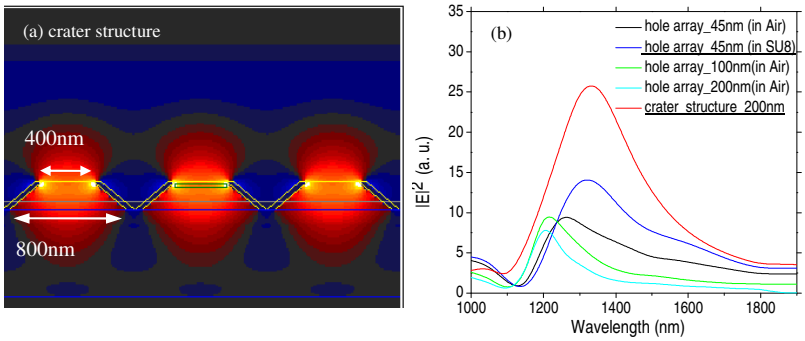

Fig. 8. (a) FDTD-simulated diagram of a crater structure having a height of 200 nm. (b) Electric field intensities determined from a near-field analysis of hole-array structures of various depths and crater structures.

To further study the electric field enhancement in 3D crater structures, we used FDTD simulations to calculate (Fig. 9) the electric field intensities at various positions (50, 100, 150, and 200 nm) within a crater cavity having a height of 200 nm. Upon increasing the position in the cavity, the electric field was enhanced from 19.1 at 50 nm to 25.9 at 200 nm; i.e., the intensity was stronger at positions closer to the top of the crater structure. We observed the strongest electric field intensity when the spacing was close near the top of the 3D hole-array structure. Because the propagation of the SPR wave occurs along the walls of the metallic cavities, decreasing the spacing of the cavity walls at the top of crater structure enhanced the transmission that was induced by the enhanced electric field intensity.

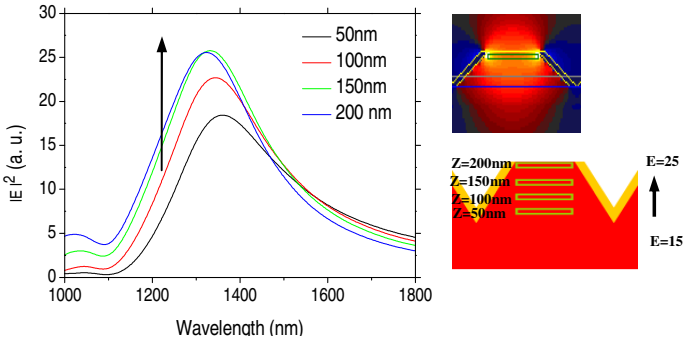

Fig. 9. Near-field simulations of the electric field intensities at distinct positions within a crater-like structure.

Figure 10 presents the experimentally measured transmission spectra of flat gold film, 2D hole-array, and crater-like hole-array structures; they agree with the FDTD-calculated results within the near-field regime. The structure-free flat gold film having a thickness of 45 nm exhibited the lowest transmittance (ca. 2.5%). The transmittance of the 2D hole-array structure was 39.9% at a wavelength of 1320 nm. We observed a significantly enhanced transmission (ca. 53.7% at 1460 nm) for the 3D crater hole-array structure. A cavity effect was evident after gradually decreasing the spacing of the cavity walls. Therefore, using this simple RIM process, we obtained a crater structure that exhibited an obvious enhancement in transmittance.

#104420 - $15.00 USD Received 21 Nov 2008; revised 17 Jan 2009; accepted 18 Jan 2009; published 27 Jan 2009

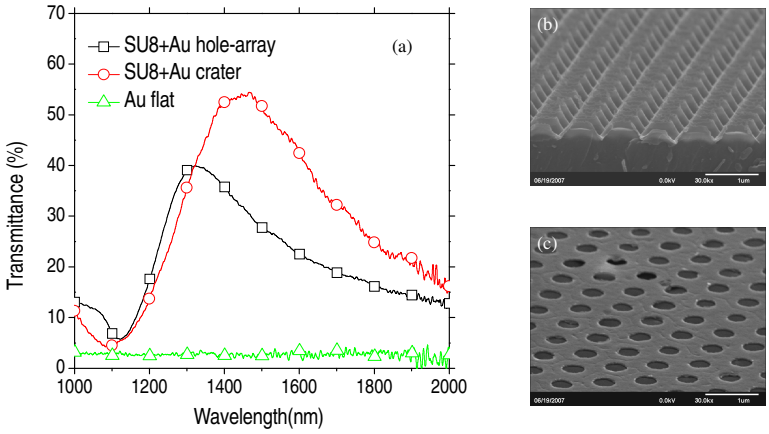

Fig. 10 (a) Transmittance spectra of flat gold film, hole-array, and crater structures. (b, c) SEM images of (b) hole-array and (c) crater-like structures.

4. Conclusion

In conclusion, we have employed a reversal imprint process to fabricate complicated 3D metal structures. Using molds of various shapes, we patterned various sub-wavelength metal structures, including pyramidal films, 2D hole-arrays, and crater-like structures. The refractive index effect provided the enhanced degrees of transmittance for the corrugated gold films. Moreover, a cavity effect was in effect, as evidenced by a comparison of the transmittance of the empty and resist-filled hole-array structures. Hole-array structures filled with resist exhibited elevated transmittance, indicating the effect of refractive index matching between the holes and their surrounding media. Furthermore, we readily fabricated crater-like 3D hole-array structures using this RIM process. The metallic craters are promising structures because of their elongated and gradually tapering cavities. From near-field analysis, we observed that the cavity effect in a crater structure significantly enhanced the intensity of optical field transmission. Experimentally obtained optical spectra confirmed the enhanced transmittance of the 3D crater structures. Using this simple RIM process allows the ready preparation of various 2D and 3D metallic structures for the application in SPR-based devices. We suspect that this RIM method will also have great potential for use in the fabrication of optical filters and semi-transmission electrodes that operate over a range of working wavelengths and transmittances.

Acknowledgments

We thank the National Science Council, Taiwan, R.O.C., for supporting this study under contracts NSC-97-2221-E-002-046-MY3 and 98-2623-E-002 -001-ET.

#104420 - $15.00 USD Received 21 Nov 2008; revised 17 Jan 2009; accepted 18 Jan 2009; published 27 Jan 2009